

1 **Optically stimulated luminescence dating of Ocean Drilling Program Core 658B:**  
2 **Complications arising from authigenic uranium uptake and lateral sediment movement.**

3  
4 S.J. Armitage\*

5  
6 Centre for Quaternary Research, Department of Geography, Royal Holloway, University of  
7 London, Egham, Surrey, TW20 0EX.

8  
9 **Abstract**

10 Ocean Drilling Program Site 658 lies under the North African summer dust plume, and ought to be  
11 an ideal target for optically stimulated luminescence (OSL) dating, since the main clastic input is  
12 far-travelled Saharan dust. However, OSL ages for coarse silt-sized quartz (40-63  $\mu\text{m}$ ) are  
13 systematically lower than independent age estimates when dose rates are calculated using a model  
14 which assumes detrital  $^{238}\text{U}$ ,  $^{232}\text{Th}$  and  $^{40}\text{K}$  and excess  $^{230}\text{Th}$  and  $^{231}\text{Pa}$ . Ages which are in good  
15 agreement with independent age control are obtained from the coarse silt samples when a correction  
16 for authigenic uranium uptake is incorporated into the dose rate model. Authigenic uranium uptake  
17 occurs under reducing conditions, which are common at the sediment-water interface, and some  
18 degree of authigenic uranium correction may be required for most marine sediments. Using this  
19 revised dose rate model, ages produced using fine silt-sized quartz (4-11  $\mu\text{m}$ ) are up to 100% older  
20 than both independent and coarse silt ages. In addition, the fine silt ages show a consistent pattern  
21 of age decrease with depth over 1.5 m of core.  $^{230}\text{Th}$  data from Site 658 indicate that this site  
22 receives 3 times more sediment laterally than vertically. It is concluded that the fine silt at Site 658  
23 contains a substantial reworked component, making it unsuitable for dating. Conversely the coarse  
24 silt fraction, which settles through water at  $\sim 40$  times the rate of fine silt, appears to be derived from  
25 dust input over the site at the time of deposition. Since prominent nepheloid (cloudy) layers occur in

---

\* e-mail: [simon.armitage@rhul.ac.uk](mailto:simon.armitage@rhul.ac.uk)

26 various deep ocean basins, and the material suspended in these layers often consists of reworked  
27 fine silt-sized sediments, coarser material should be dated where possible.

28

29 *Keywords:* Optically stimulated luminescence; Geochronology; Marine sediments; North Africa.

30

## 31 **1. Introduction**

32 Marine sediments are one of the most widely exploited archives of palaeoenvironmental information.

33 At present, most chronologies are constructed by tuning marine proxies for global ice volume ( $\delta^{18}\text{O}$ )

34 to the well understood variations in the Earth's orbit (Lisiecki and Raymo, 2005), by the identification

35 of event horizons (e.g. Sikes et al., 2000) and/or by radiocarbon dating. However, dating deep-sea

36 sediments remains problematic. Chronologies based on  $\delta^{18}\text{O}$  records are dependent upon the accuracy

37 of the climate change model assumed and necessarily obscure information regarding phasing of the

38 events observed. Event horizons are only useful where their occurrence is reasonably frequent in the

39 time period of interest. In addition, both techniques require approximately continuous sedimentation,

40 and the absence of sediment reworking. Whilst a tremendously powerful geochronological tool,

41 Accelerator Mass Spectrometry (AMS) radiocarbon dating is limited to the last 50-60,000 years and

42 is subject to uncertainties due to variation in the atmospheric  $^{14}\text{C}$  concentrations and the marine

43 carbon reservoir. The latter effect may introduce a substantial and temporally variable systematic

44 error to a chronology (Sikes et al., 2000). In addition, chronologies can only be constructed using

45 radiocarbon or the  $\delta^{18}\text{O}$  record where organic carbonates are preserved, which is not the case in areas

46 with high clastic sedimentation rates (Sugisaki et al., 2010), or at sites below the carbonate

47 compensation depth. These limitations to well established dating techniques have led several authors

48 (Berger, 2006; Jakobsson et al., 2003; Stokes et al., 2003) to advocate the use of optically stimulated

49 luminescence (OSL) methods to provide age control for deep-sea sediments.

50

51 Although marine sediments were first dated using thermoluminescence techniques in 1979 (Wintle  
52 and Huntley, 1979) and using OSL techniques in 2003 (Jakobsson et al., 2003; Stokes et al., 2003),  
53 there are relatively few published luminescence chronologies for open ocean sediments. This absence  
54 is possibly explained by the complex dose rate measurements and calculations required, due to the  
55 presence of uranium-series disequilibrium in many deep sea sediments (Wintle and Huntley, 1979).  
56 For many terrestrial sediments it is valid to assume that the  $^{238}\text{U}$ ,  $^{235}\text{U}$  and  $^{232}\text{Th}$  decay series are in  
57 secular equilibrium. Consequently, dose rates due to these decay series are effectively invariant over  
58 Quaternary timescales. This remains true for  $^{232}\text{Th}$  in marine sediments since thorium is highly  
59 insoluble and is incorporated into marine sediments, in equilibrium with its daughters, within the  
60 detrital component. Conversely, the geochemistry of both uranium decay series makes it likely that  
61 they will be in disequilibrium in late Quaternary ocean sediments. In the oxidising conditions found  
62 in most seawater, uranium is highly soluble. However, long-lived isotopes in both uranium decay  
63 series ( $^{230}\text{Th}$  in the  $^{238}\text{U}$  series and  $^{231}\text{Pa}$  in the  $^{235}\text{U}$  series) are insoluble and are removed from the  
64 water column by sorption to the surface of settling particles (Henderson and Anderson, 2003)  
65 meaning that they are initially found in excess (relative to isotopes earlier in the relevant decay series)  
66 in many marine sediments. These isotopes have half-lives which are similar to the timescales over  
67 which OSL dating is applicable (75 and 32.8 ka for  $^{230}\text{Th}$  and  $^{231}\text{Pa}$  respectively) causing the dose  
68 rate due to these isotopes and their decay products to evolve as the sediment ages. Consequently, OSL  
69 dating of marine sediments is complicated by the need to demonstrate the absence of excess activity  
70 in the uranium decay series (Jakobsson et al., 2003; Sugisaki et al., 2010; Sugisaki et al., 2012) or to  
71 quantify excess activity and incorporate the resulting time-dependant dose rate changes into age  
72 calculations (Stokes et al., 2003; Wintle and Huntley, 1979). This study compares AMS  $^{14}\text{C}$  and  
73 quartz OSL chronologies produced for a core from Ocean Drilling Program (ODP) Site 658.

74

## 75 **2 Materials and methods**

76 Core 658B was the second of three cores recovered from a water depth of 2,263 m off Cap Blanc,  
77 Mauritania (20°45'N, 18°35'W) during ODP Leg 108 (Ruddiman et al., 1988). Trade winds cause  
78 strong upwelling over the site, leading to high surface productivity and high biogenic particle fluxes  
79 to the seafloor. Biogenic carbonate comprises 40-60% by mass of the sediment, with the remainder  
80 being terrigenous dust (deMenocal et al., 2000). The high terrigenous dust flux is due to the site's  
81 location beneath the axis of the summer African dust plume (Figure 1). Core 658B is an ideal target  
82 for testing OSL dating in the marine realm since: (1) It has a high accumulation rate (c.18 cm/ka,  
83 deMenocal et al., 2000); (2) Terrigenous dust input should provide a substantial well-bleached  
84 quartz component; (3) Neighbouring core 658C has a well dated dust flux record covering the last  
85 22 ka (deMenocal et al., 2000) and (4) the excess  $^{230}\text{Th}$  ( $^{230}\text{Th}_{\text{xs}}$ ) record for core Core 658C (Adkins  
86 et al., 2006) may be used to calculate excess activity in Core 658B.

87  
88 Independent chronological data for Core 658B were obtained from two sources. Firstly, 18 samples  
89 from core depths ranging from ~2.3-10.9 m (effectively the upper ~8.5 m of core since the  
90 uppermost 2.3 m appears to replicate underlying material) were dated by AMS  $^{14}\text{C}$  on 150-250  $\mu\text{m}$   
91 *Globigerinoides bulloides* tests. Fifteen of these AMS  $^{14}\text{C}$  measurements yielded finite ages (Table  
92 S1). Secondly, dated stratigraphic markers in Core 658C (deMenocal et al., 2000) and the LR04  
93 benthic  $\delta^{18}\text{O}$  stack (Lisiecki and Raymo, 2005) were identified in Core 658B (Table S2). Both  
94 approaches yield a similar age-depth relationship, though the Core 658B AMS  $^{14}\text{C}$  ages show age  
95 inversions especially below 7 m, towards the upper limit of the technique (Figure 2). There is no  
96 apparent lithological change at 7 m, and it is possible that the age inversions are due to reworking of  
97 foraminiferal tests or variable reservoir effects.

98

## 99 **2.1 Equivalent dose determination**

100 Samples were obtained from a 66 mm diameter split core at the ODP East Coast Repository,  
101 Lamont-Doherty Earth Observatory, USA. Since collection in 1986, the core had been refrigerated

102 and kept moist via damp sponges inserted at the ends of each core section, but no attempt had been  
103 made to shield the core from light. Paired samples were taken every ~25 cm through the uppermost  
104 11 m of the core by inserting short sections of 20 mm diameter opaque tubing. Under subdued  
105 orange lighting the sediment was extruded and the outer ~8 mm was discarded to avoid core barrel  
106 smearing. The light exposed upper ~8 mm was removed and used for carbonate content and dose  
107 rate analysis. The middle ~8 mm of the sample was dispersed in deionised water and sieved at 150  
108  $\mu\text{m}$ , with the  $>150$  fraction consisting of foraminiferal tests, and the  $<150$   $\mu\text{m}$  fraction being used  
109 for dating. The dating fraction was sequentially treated with HCl, H<sub>2</sub>O<sub>2</sub> and H<sub>2</sub>SiF<sub>6</sub> to remove  
110 carbonate, organic matter and feldspars respectively. The resulting mixture was separated into fine  
111 silt (4-11  $\mu\text{m}$ ) and coarse silt (40-63  $\mu\text{m}$  where present) fractions via Stokes settling and wet sieving  
112 respectively.

113

114 All OSL measurements presented in this study were carried out using a Risø TL/OSL-DA-15  
115 automated dating system (Bøtter-Jensen et al., 2000). Optical stimulation of single aliquots was  
116 carried out using a blue ( $470 \pm 30$  nm) light emitting diode (LED) array with a nominal power density  
117 of 18 mW/cm<sup>2</sup>. Infra-red (IR) stimulation was carried out using an IR (870 nm) laser diode array.  
118 OSL was measured using an Electron Tubes Ltd 9235QB photomultiplier tube with 7.5 mm of Hoya  
119 U-340 filter interposed between the sample and photomultiplier. Irradiation was carried out using a  
120 40 mCi <sup>90</sup>Sr/<sup>90</sup>Y beta source, calibrated relative to the National Physical Laboratory, Teddington  
121 Hotspot 800 <sup>60</sup>Co  $\gamma$ -source (Armitage and Bailey, 2005). Single-aliquot equivalent doses ( $D_e$ ) were  
122 determined using the single-aliquot regenerative-dose (SAR) method (Galbraith et al., 1999; Murray  
123 and Wintle, 2000). OSL signals were measured at 125 °C and growth curves were fitted using a  
124 saturating exponential function. No dependence of  $D_e$  upon preheating regime was found (Figure S1)  
125 and a preheating regime of 260 °C, 10 s for PH1 (the pre-heat prior to measurement of  $L_n$  or  $L_x$ ) and  
126 220 °C, 10 s for PH2 (the pre-heat prior to measurement of  $T_n$  or  $T_x$ ) was adopted for subsequent  
127 measurements. Dose recovery experiments (Roberts et al., 1999; Wallinga et al., 2000) were

128 performed on the coarse silt fractions of samples 11B, 19A and 27A ( $D_e = 23, 44$  and  $77$  Gy  
129 respectively) using this preheating regime, yielding dose recovery ratios of  $0.99 \pm 0.01$ ,  $0.98 \pm 0.01$   
130 and  $0.98 \pm 0.01$  respectively. When calculating  $D_e$ , aliquots were rejected where the recycling ratio  
131 (Murray and Wintle, 2000) or IR depletion ratio (Duller, 2003) differed from unity by more than two  
132 standard deviations, or where the sensitivity corrected luminescence intensity in response to a 0 Gy  
133 regeneration dose exceeded 5% of the sensitivity corrected natural luminescence intensity (Table S3).

134

## 135 **2.2 Dose rate determination**

136 The environmental dose rate for samples from core 658B consists of alpha, beta and gamma  
137 components, since the overlying water completely shields the ocean floor sediments from cosmic  
138 rays.  $^{238}\text{U}$  and  $^{232}\text{Th}$  and bulk K concentrations were measured using ICP-MS (Table S4). Burial  
139  $^{230}\text{Th}_{\text{xs}}$  for all samples was assumed to be the mean value ( $36.6 \pm 9.3$  Bq/kg) measured by Adkins et  
140 al. (2006) for Core 658C over the time period 2-18.5 ka. Adkins et al. (2006) determined  $^{230}\text{Th}_{\text{xs}}$   
141 using a VG Plasma Quad 2 ICP-MS, reporting <1% counting statistics errors and 0.17 Bq/kg  
142 procedural blanks. Initial  $^{231}\text{Pa}_{\text{xs}}$  ( $3.38 \pm 0.87$  Bq/kg) was calculated using the 0.093 production  
143 activity ratio of  $^{231}\text{Pa}/^{230}\text{Th}$  (Henderson and Anderson, 2003). Time independent dose rates were  
144 calculated from  $^{238}\text{U}$  and  $^{232}\text{Th}$  and K concentrations, assuming equilibrium in both decay series,  
145 using the standard conversion factors (Adamiec and Aitken, 1998). The additional time dependant  
146 dose contribution due to  $^{230}\text{Th}_{\text{xs}}$  and  $^{231}\text{Pa}_{\text{xs}}$ , and the final age calculation, were performed using the  
147 method outlined by Stokes et al. (2003). Both coarse and fine silt dose rates were corrected for  
148 alpha efficiency ( $0.04 \pm 0.02$ ), alpha and beta attenuation and water content (Aitken, 1985). Water  
149 contents were taken from the relevant ODP initial report (Ruddiman et al., 1988). The above dose  
150 rate calculation is referred to as the “Marine<sub>xs</sub>” dose rate model hereafter. Dose rates and ages  
151 calculated using the Marine<sub>xs</sub> model are presented in Table S5.

152

## 153 **3 Results and discussion**

154 Coarse silt OSL ages calculated using the Marine<sub>xs</sub> model are shown alongside the independent  
155 chronological data in Figure 2. It is clear that the coarse silt OSL ages underestimate the  
156 independent ages by a considerable amount.

157

158 Whilst uranium forms soluble species in oxidising conditions, under suboxic or anoxic conditions it  
159 is reduced to its insoluble tetravalent state (Henderson and Anderson, 2003). This situation  
160 frequently occurs at or near the sediment-water interface, resulting in the incorporation of  
161 authigenic uranium in marine sediments. Especially high authigenic uranium concentrations occur  
162 where high surface productivity leads to a high organic matter flux to the sea bed, since this  
163 material consumes oxygen during its decay (Henderson and Anderson, 2003). Consequently it  
164 might be expected that sediments from ODP site 658 will have a high authigenic uranium content.  
165 Authigenic uranium isotopes ( $^{238}\text{U}_{\text{auth}}$  and  $^{234}\text{U}_{\text{auth}}$ ) are incorporated into marine sediment at the  
166 seawater activity ratio of  $^{234}\text{U}/^{238}\text{U} = 1.146$  (Robinson et al., 2004), and without any supported  
167 decay products. For dating purposes,  $^{238}\text{U}_{\text{auth}}$  instantly attains equilibrium with the next two decay  
168 products ( $^{234}\text{Th}$  and  $^{234}\text{Pa}$ ) since neither is long-lived. Conversely,  $^{234}\text{U}$  has a half-life of 245 ka and  
169 hence will not approach equilibrium with its parent ( $^{238}\text{U}$ ) over the applicable age range of quartz  
170 OSL dating. However, since authigenic uranium is incorporated into the sediment at an activity  
171 ratio of  $^{234}\text{U}/^{238}\text{U}$  of 1.146,  $^{234}\text{U}_{\text{auth}}$  may be treated as being in equilibrium with  $^{238}\text{U}_{\text{auth}}$  for the  
172 purposes of estimating dose rates. The slight excess activity of  $^{234}\text{U}_{\text{auth}}$  over  $^{238}\text{U}_{\text{auth}}$  has a negligible  
173 impact upon dose rates since the decay of  $^{234}\text{U}$  contributes a small proportion of the dose rate due to  
174 the  $^{238}\text{U}$  decay series (11% of alpha, 0.5% of beta and 0.1% of gamma). Since both  $^{234}\text{U}$  and its  
175 decay product  $^{230}\text{Th}$  are long-lived (half-lives of 245 and 75 ka respectively), the ingrowth of  
176  $^{234}\text{U}_{\text{auth}}$  decay products is negligible over the 0-50 ka timeframe covered by this study.

177 Consequently, in this study the dose rate due to authigenic uranium may be approximated by  
178 assuming secular equilibrium from  $^{238}\text{U}_{\text{auth}}-^{234}\text{U}_{\text{auth}}$ , and no dose from the decay products of  $^{234}\text{U}_{\text{auth}}$ .  
179 Since most of the alpha, beta and gamma energy in the  $^{238}\text{U}$  decay series is emitted at or below  $^{234}\text{U}$

180 (Stokes et al., 2003), the dose rate must be corrected to account for authigenic uranium uptake  
181 where it occurs.

182

183 The authigenic uranium content of a marine sediment may be calculated from the measured  $^{238}\text{U}$   
184 and  $^{232}\text{Th}$  activities (or the activities calculated from the measured concentrations), since the  $^{232}\text{Th}$   
185 is entirely detrital, and the  $^{238}\text{U}/^{232}\text{Th}$  activity ratio of crustal rocks and pelagic marine sediments is  
186  $0.8\pm 0.2$  (Anderson et al., 1989). Equation 1 was used to calculate authigenic uranium contents of  
187 Core 658B samples

188

$$189 \quad U_{\text{auth}} = {}^{238}\text{U}_m - 0.8 * {}^{232}\text{Th}_m \quad (\text{Eq. 1})$$

190

191 where  $^{238}\text{U}_m$  and  $^{232}\text{Th}_m$  are the measured activities of  $^{238}\text{U}$  and  $^{232}\text{Th}$  respectively (Yu et al., 1999).  
192 This calculation was performed for all samples in this study (n=29), adding a 20% uncertainty to the  
193  $U_{\text{auth}}$  activity, and the mean  $^{238}\text{U}_{\text{auth}}/^{238}\text{U}_m$  ratio was  $0.77\pm 0.18$ . In the  $\text{Marine}_{\text{xs}}$  dose rate model, the  
194 entire detrital  $^{238}\text{U}$  decay series is assumed to be in equilibrium, which will result in an overestimate  
195 of the true dose rate due to uranium where authigenic uranium uptake has occurred. Ages were  
196 recalculated using the revised “ $\text{Marine}_{\text{xs+auth}}$ ” dose rate model, in which the dose rate due to  $^{238}\text{U}_{\text{auth}}$   
197 is calculated assuming equilibrium to  $^{234}\text{U}$ , with no dose from the decay products of  $^{234}\text{U}_{\text{auth}}$ , and the  
198 detrital  $^{238}\text{U}$  ( $^{238}\text{U}_m - ^{238}\text{U}_{\text{auth}}$ ) decay series is assumed to be in equilibrium throughout. In the  
199  $\text{Marine}_{\text{xs+auth}}$  dose rate model, all other components are calculated as in the  $\text{Marine}_{\text{xs}}$  dose rate  
200 model. Coarse silt OSL ages calculated using the  $\text{Marine}_{\text{xs+auth}}$  dose rate model (Table S6) are in  
201 good agreement with the independent chronological data (Figure 3a), indicating that the age  
202 underestimation observed when using the  $\text{Marine}_{\text{xs}}$  dose rate model is caused by the failure of this  
203 model to account for authigenic uranium uptake. The mean ratio of  $\text{Marine}_{\text{xs}}/ \text{Marine}_{\text{xs+auth}}$  dose rate  
204 ages is  $0.73\pm 0.05$ .

205



206 Ages were calculated, using the Marine<sub>e<sub>xs</sub>+auth</sub> dose rate model, for the 16 samples for which  
207 equivalent doses had been measured on fine quartz silt (Table S7, Figure 3b). The fine silt ages do  
208 not increase monotonically with depth, nor do they agree with the independent chronological data  
209 or the paired coarse silt ages where available (~4-6.5 m). All fine silt OSL ages are older than  
210 corresponding coarse silt OSL ages and independent age control. Together these discrepancies are  
211 taken to indicate that the dose rate model is correct, but that the fine silt equivalent doses do not  
212 represent the dose experienced since the deposition of these particles at ODP Site 658. It has been  
213 suggested that in many marine contexts coarse silt might be preferential to fine silt for dating since  
214 90% of grains within the nepheloid (cloudy) layer in non-polar deep oceans, which results from  
215 sediment reworking, consist of grains with a diameter of 0.5-8.5  $\mu\text{m}$  (Berger, 2006). Also, the  
216  $^{230}\text{Th}_{\text{xs}}$  record from ODP core 658C indicates that over the last 20 ka, this site has received 3 times  
217 more sediment laterally than vertically, though this ratio is quite variable (Adkins et al., 2006).  
218 Since 50  $\mu\text{m}$  grains settle through water at ~40 times the rate of 8  $\mu\text{m}$  grains, the coarse silt fraction  
219 is more likely to be incorporated via sea surface aeolian input immediately prior to deposition than  
220 is the fine silt fraction. Consequently, the discrepancy between coarse silt and fine silt OSL ages at  
221 site 658B is attributed to ocean floor reworking, without exposure to sunlight, of the latter.

222

#### 223 **4 Conclusions**

224 Disequilibrium in the  $^{238}\text{U}$  and  $^{235}\text{U}$  decay series due to precipitation of insoluble isotopes from the  
225 water column is a well-known phenomenon in marine sediments (Wintle and Huntley, 1979). With  
226 appropriate  $^{230}\text{Th}_{\text{xs}}$  measurements, the effect of this disequilibrium on dose rates can be accounted  
227 for (Stokes et al., 2003). At ODP Site 658, authigenic uranium uptake represents an important  
228 additional source of disequilibrium. A simple dose rate correction is proposed, which appears  
229 suitable for sediments which are much younger than the half-life of  $^{234}\text{U}$ . However, more complex  
230 dose rate corrections will be required in older samples where significant ingrowth of  $^{234}\text{U}_{\text{auth}}$  decay  
231 products has occurred. It is probable that authigenic uranium uptake in marine sediments could

232 disguise quite large  $^{230}\text{Th}_{\text{xs}}$  activities where secular equilibrium is diagnosed on the basis of  
233  $^{226}\text{Ra}/^{238}\text{U}$  activity ratios determined using high-resolution gamma spectrometry (e.g. Jakobsson et  
234 al., 2003). Consequently, it is prudent to calculate authigenic uranium uptake for all samples when  
235 dating open ocean sediments.

236

237 Coarse silt (40-63  $\mu\text{m}$ ) OSL ages from site 658B are internally consistent and in good agreement  
238 with independent age control. Conversely, fine silt (4-11  $\mu\text{m}$ ) yielded older ages for all samples,  
239 and dates did not increase monotonically with depth. It appears likely that seafloor reworking of  
240 fine silt caused these ages to be unrepresentative of the timing of sediment formation at the sampled  
241 position. This result potentially limits the applicability of OSL dating to marine sediments, since the  
242 coarse silt component at site 658B results from its location under the North African summer dust  
243 plume. However, since the deep ocean nepheloid layer contains little material  $>10 \mu\text{m}$ , it is possible  
244 that accurate ages for sediment formation could be obtained from silts only slightly coarser than the  
245 4-11  $\mu\text{m}$  fraction measured here.

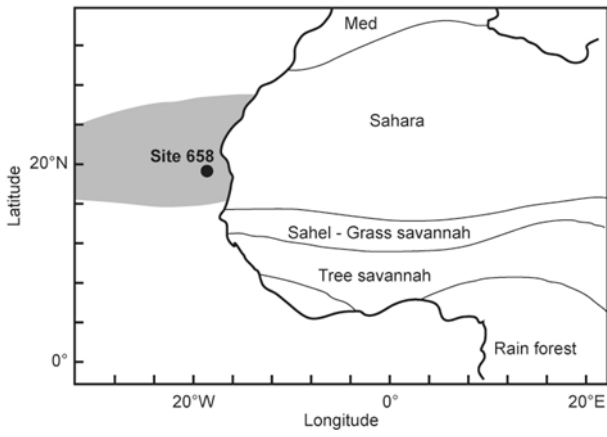
246

## 247 **5 Acknowledgements**

248 The measurements presented in the paper were funded by NERC grant NER/T/S/2001/01236 and  
249 NERC Radiocarbon Analysis Allocation No. 1036.0403, both awarded to Stephen Stokes. Calcium  
250 carbonate analysis and foraminifera picking for  $^{14}\text{C}$  and  $\delta^{18}\text{O}$  measurements was carried out by  
251 Chris Beer and Abigail Stone. Jenny Kynaston drew Figure 1. Andreas Lang is thanked for  
252 providing a constructive review. This work was initiated by Stephen Stokes, to whom the paper is  
253 dedicated.

254 **Figures**

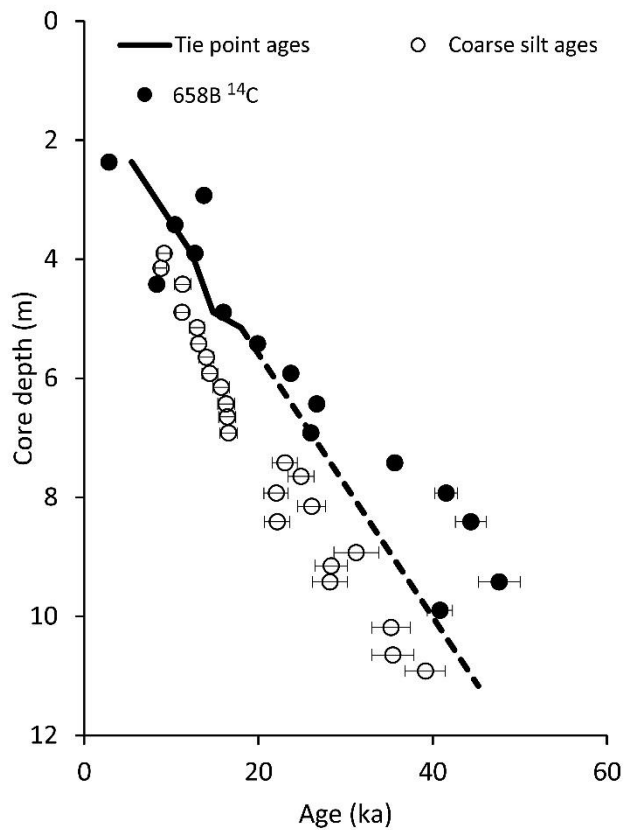
255



256

257 Figure 1: Location of ODP Site 658 under the summer African dust plume (grey). Redrawn from  
258 deMenocal et al. (2000).

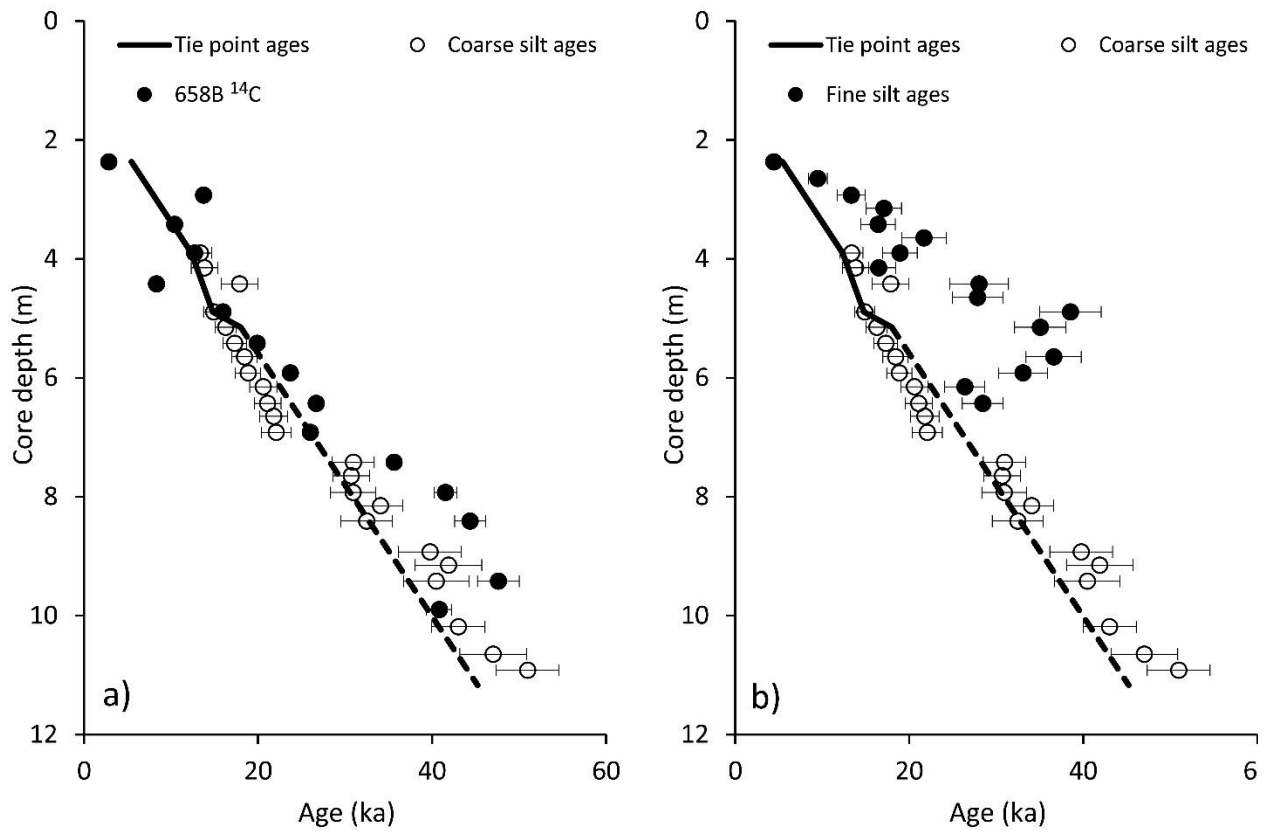
259



260

261 Figure 2: Chronological models for Core 658B. Filled circles represent independent age estimates  
 262 determined using AMS <sup>14</sup>C on foraminifera from Core 658B and the solid line represents an age-  
 263 depth relationship determined by matching stratigraphic events to external dated stratigraphies,  
 264 assuming constant sedimentation between these tie points. The dashed line represents the age-depth  
 265 relationship beyond 18 ka, assuming that the 22 cm/ka sedimentation rate observed between 2.37  
 266 and 5.15 m core depth continues. Open circles represent coarse silt OSL ages calculated using the  
 267 Marine<sub>xs</sub> dose rate model.

268



269 Figure 3: Independent age estimates and OSL ages for Core 658B. a) Independent age estimates and  
 270 coarse silt OSL ages calculated using the Marine<sub>xs+auth</sub> dose rate model. b) Coarse silt and fine silt  
 271 OSL ages calculated using the Marine<sub>xs+auth</sub> dose rate model, plotted alongside the independent age-  
 272 depth model. Core 658B AMS <sup>14</sup>C ages have been removed from panel b for clarity.  
 273

274 **References**

275

276 Adamiec, G., Aitken, M., 1998. Dose-rate conversion factors: update. *Ancient TL* 16, 37-50.

277 Adkins, J., deMenocal, P., Eshel, G., 2006. The "African humid period" and the record of marine  
278 upwelling from excess  $^{230}\text{Th}$  in Ocean Drilling Program Hole 658C. *Paleoceanography* 21.

279

280 Aitken, M.J., 1985. *Thermoluminescence dating*. Academic press.

281

282 Anderson, R.F., LeHuray, A.P., Fleisher, M.Q., Murray, J.W., 1989. Uranium deposition in saanich  
283 inlet sediments, vancouver island. *Geochimica et Cosmochimica Acta* 53, 2205-2213.

284

285 Armitage, S.J., Bailey, R.M., 2005. The measured dependence of laboratory beta dose rates on  
286 sample grain size. *Radiat Meas* 39, 123-127.

287

288 Berger, G.W., 2006. Trans-arctic-ocean tests of fine-silt luminescence sediment dating provide a  
289 basis for an additional geochronometer for this region. *Quaternary Science Reviews* 25, 2529-2551.

290

291 Bøtter-Jensen, L., Bulur, E., Duller, G.A.T., Murray, A.S., 2000. Advances in luminescence  
292 instrument systems. *Radiat Meas* 32, 523-528.

293

294 deMenocal, P., Ortiz, J., Guilderson, T., Adkins, J., Sarnthein, M., Baker, L., Yarusinsky, M., 2000.  
295 Abrupt onset and termination of the African Humid Period: Rapid climate responses to gradual  
296 insolation forcing. *Quaternary Science Reviews* 19, 347-361.

297

298 Duller, G.A.T., 2003. Distinguishing quartz and feldspar in single grain luminescence  
299 measurements. *Radiat Meas* 37, 161-165.

300

301 Galbraith, R.F., Roberts, R.G., Laslett, G.M., Yoshida, H., Olley, J.M., 1999. Optical dating of  
302 single and multiple grains of quartz from Jinmium rock shelter, northern Australia: Part I,  
303 experimental design and statistical models. *Archaeometry* 41, 339-364.

304

305 Henderson, G.M., Anderson, R.F., 2003. The U-series toolbox for palaeoceanography, in: Bourdon,  
306 B., Henderson, G.M., Lundstrom, C.C., Turner, S.P. (Eds.), *Uranium-series geochemistry*.  
307 *Geochemical Society and Mineralogical Society of America*, Washington, p. 656.

308

309 Jakobsson, M., Backman, J., Murray, A., Løvlie, R., 2003. Optically stimulated luminescence  
310 dating supports central arctic ocean cm-scale sedimentation rates. *Geochemistry, Geophysics,*  
311 *Geosystems* 4.

312

313 Lisiecki, L.E., Raymo, M.E., 2005. A Pliocene-Pleistocene stack of 57 globally distributed benthic  
314  $\delta^{18}\text{O}$  records. *Paleoceanography* 20, 1-17.

315

316 Murray, A.S., Wintle, A.G., 2000. Luminescence dating of quartz using an improved single-aliquot  
317 regenerative-dose protocol. *Radiat Meas* 32, 57-73.

318

319 Roberts, R.G., Galbraith, R.F., Olley, J.M., Yoshida, H., Laslett, G.M., 1999. Optical dating of  
320 single and multiple grains of quartz from Jinmium rock shelter, northern Australia: Part II, results  
321 and implications. *Archaeometry* 41, 365-395.

322

323 Robinson, L.F., Belshaw, N.S., Henderson, G.M., 2004. U and Th concentrations and isotope ratios  
324 in modern carbonates and waters from the Bahamas. *Geochimica et Cosmochimica Acta* 68, 1777-  
325 1789.

326 Ruddiman, W., Sarnthein, M., Baldauf, J., al., e., 1988. Proceedings of the Ocean Drilling Program  
327 Part A - Initial Reports.  
328

329 Sikes, E.L., Samson, C.R., Guilderson, T.P., Howard, W.R., 2000. Old radiocarbon ages in the  
330 southwest Pacific Ocean during the last glacial period and deglaciation. *Nature* 405, 555-559.  
331

332 Stokes, S., Ingram, S., Aitken, M.J., Sirocko, F., Anderson, R., Leuschner, D., 2003. Alternative  
333 chronologies for Late Quaternary (Last Interglacial-Holocene) deep sea sediments via optical dating  
334 of silt-sized quartz. *Quaternary Science Reviews* 22, 925-941.  
335

336 Sugisaki, S., Buylaert, J.P., Murray, A., Tsukamoto, S., Nogi, Y., Miura, H., Sakai, S., Iijima, K.,  
337 Sakamoto, T., 2010. High resolution OSL dating back to MIS 5e in the central Sea of Okhotsk.  
338 *Quat Geochronol* 5, 293-298.  
339

340 Sugisaki, S., Buylaert, J.P., Murray, A.S., Harada, N., Kimoto, K., Okazaki, Y., Sakamoto, T.,  
341 Iijima, K., Tsukamoto, S., Miura, H., Nogi, Y., 2012. High resolution optically stimulated  
342 luminescence dating of a sediment core from the southwestern Sea of Okhotsk. *Geochemistry,*  
343 *Geophysics, Geosystems* 13.  
344

345 Wallinga, J., Murray, A., Duller, G., 2000. Underestimation of equivalent dose in single-aliquot  
346 optical dating of feldspars caused by preheating. *Radiat Meas* 32, 691-695.

347 Wintle, A.G., Huntley, D.J., 1979. Thermoluminescence dating of a deep-sea sediment core. *Nature*  
348 279, 710-712.  
349

350 Yu, E.F., Liang, C.H., Chen, M.T., 1999. Authigenic uranium in marine sediments of the Benguela  
351 current upwelling region during the last glacial period. *Terrestrial, Atmospheric and Oceanic*  
352 *Sciences* 10, 201-214.  
353